SPACECRAFT ATOMIC CLOCK FLIGHT SIMULATION AND TEST STATION

H. Wang, J. C. Camparo, and G. Iyanu
The Aerospace Corporation
PO Box 92957, MS 2-253
Los Angeles, California 90009-2957
Tel: (310)336-5863
he.wang@aero.org

Abstract

In order to help satellite operators understand and resolve flight atomic clock issues, we have constructed a flight simulation and test facility to assess and investigate the behavior of flight-model atomic clocks in a simulated operational space environment. To date, this capability has been focused primarily on exercising the atomic clocks flown by Milstar and AEHF satellites. In this paper, without going into the requirements or capabilities of the Milstar/AEHF systems, we describe our test station and report on some recent results regarding the simulated space performance of Rb atomic frequency standards (RAFS). The "space segment" of the test station has two spacecraft clocks housed in vacuum chambers. Each clock's DC power supply and bath-circulator controlled thermal plate simulates the satellite's power bus and the satellite's diurnal temperature variations, respectively. The "ground control" segment includes a multiple clock measurement system, and a data acquisition and command interface system. Not only can we measure each clock's telemetry signals and output frequency while the clocks operate in vacuum, we are also able to send commands to each clock. For example, we can switch a RAFS between its "atomic-clock" mode and its "crystal-oscillator-backup" mode, and we can command a frequency update to a RAFS in order to synchronize the clock while we monitor the effects of the command on the clock's output frequency and telemetry. We believe that the capabilities of our simulation and test station will be of interest to the sponsors and attendees of the conference.

INTRODUCTION AND THE TEST STATION

Atomic clocks now have a fairly well-established history as spacecraft time and frequency reference devices in global navigation satellite systems (GNSS) and communication satellite systems **[1-6]**. Nevertheless, ground operators for satellites carrying atomic clocks will have questions regarding the nominal behavior and operational characteristics of the flight clocks as they attempt to resolve on-orbit anomalies and make operational decisions. For example, ground operators might want to know the temperature sensitivity of a Milstar satellite's rubidium master oscillator (RMO) when it operates in crystal-oscillator-backup mode as opposed to atomic-clock mode; or they might want to know the frequency retrace of an RMO switching between atomic-clock mode and crystal-oscillator-backup mode (The definition of these two Milstar RMO modes will be made clearer in what follows.). Further, when satellite operators perform a frequency update operation, they might want to know how a satellite atomic clock behaves following a change to the onboard clock's digital frequency tuning word. Though answers to these questions can sometimes be obtained by examining archived pre-flight test data (e.g., the RMO's temperature sensitivity), other questions can prove more problematic because pre-flight data may not exist or the flight clock issue may deal with a specific operational scenario **[4,6-7]**. In order to help satellite operators understand and resolve these flight atomic clock issues, we have constructed a flight simulation

and test station to assess and investigate the behavior of flight-model atomic clocks in a simulated operational space environment.

Our simulation and test station is shown as a block diagram in Figure 1. At present, two Milstar rubidium master oscillators, RMO-15 and RMO-3, manufactured by Frequency Electronics, Inc. (FEI) have been placed in a vacuum chamber that is pumped down to a pressure of 3×10^{-6} atm. Each RMO unit is mounted on a bath-circulator controlled thermal plate in the chamber, so that we are able to simulate a satellite's diurnal temperature variations. Not only can we monitor all telemetry signals while the clock is operating in vacuum at an analog-to-digital resolution exceeding that of any actual space-to-ground signal; we are also able to command the clock, e.g., to switch the clock between RMO mode and crystal oscillator backup mode, and to command a frequency update while monitoring the effects of the command on the clock's frequency and telemetry signals. In our test station, each RMO unit is powered by a constant-voltage DC power supply that simulates the satellite power bus. The output frequency of the Rb clocks is measured using a multiple clock measurement system against three reference clocks: a Cs clock (Symmetricom 4065C/075), an independent Rb clock (Symmetricom 8130A) and a crystal oscillator clock (Datum 1000B). Our Cs clock is regularly calibrated with a GPS receiver against UTC(GPS). The four clock measurement system gives us the option to assess the performance of the RMOs using a 3-cornered hat technique **[8-9]**. The RMO's frequency is tuned with a 16-bit frequency control word command, generated using a PC based serial peripheral interface (SPI) bus.

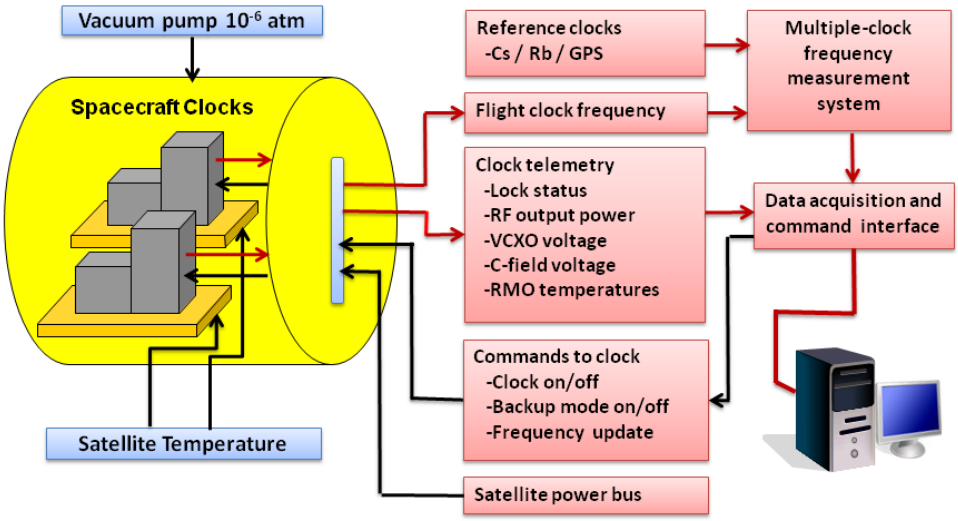

Figure 1. Block diagram of our atomic clock flight simulation and test station.

Figure 2 and Figure 3 provide two examples of telemetry and frequency measurements with our station. Shown in Figure 2 are seven telemetry data channels recorded from RMO-15 as the RMO is switched from its crystal-oscillator backup mode to its atomic-clock or RMO mode around t = 110 sec. When the transition occurs, the clock's phase lock loop (PLL) status (the black line) telemetry output jumps from LO to HI and the VCXO voltage goes through a change in order to lock the VCXO to the atomic reference

transition. In Figure 3 we plot the measured RMO output frequency as a function of the frequency control word (FCW) as we fine-tune the clock near the operating point FCW = 32768 (8000 in hexadecimal), demonstrating the remote frequency-tuning capability of the simulation and test facility.

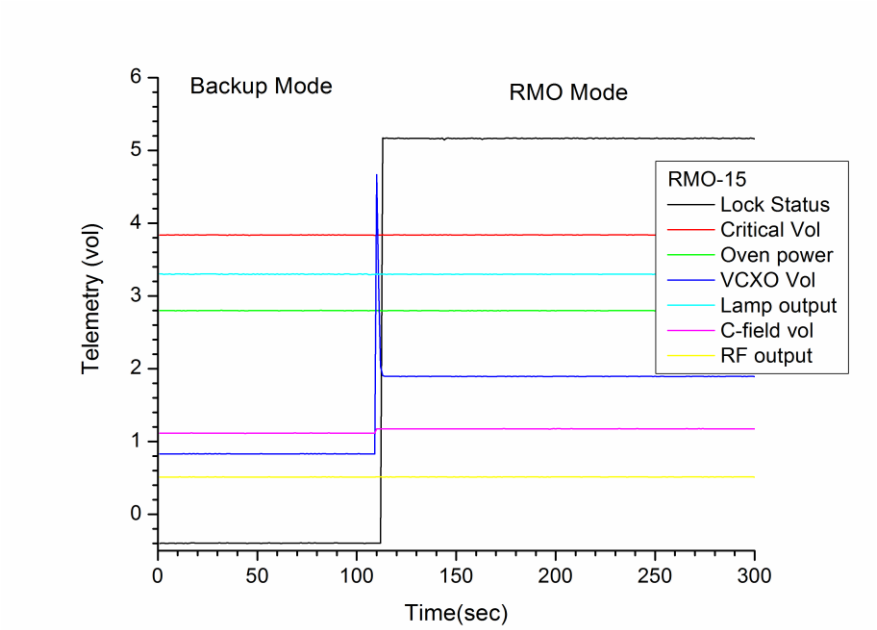

Figure 2. Example of recorded RMO telemetry data. At t = 110 s, the clock is switched to its RMO mode from its crystal oscillator backup mode.

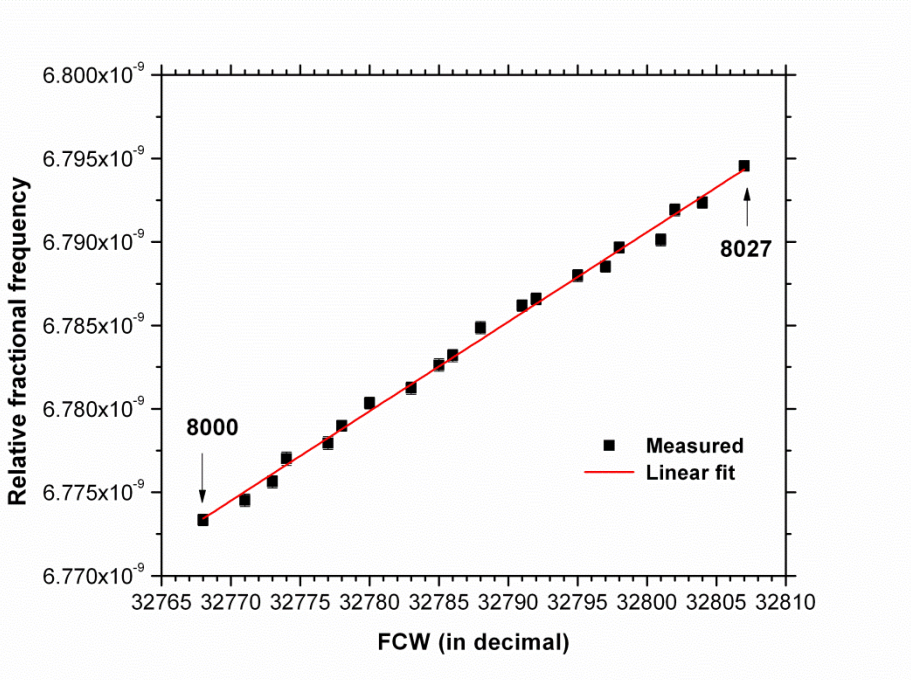

Figure 3. Example of measured relative fractional frequency of RMO-3 near FCW = 32768 (8000 in hexadecimal) when the clock is fine-tuned.

Figure 4 shows the Allan deviation of RMO-15 when operating in vacuum. The Allan variance was calculated using measured frequency data with a 3-cornered-hat algorithm as given in Equation (1). Briefly, if we let σ_i^2 stand for the theoretical frequency-variance of the i^{th} clock, independent of any reference, and σ_{ij}^2 the *measured* variance of the i^{th} clock when using the j^{th} clock as a reference, then (assuming no correlation between the i^{th} and j^{th} clocks' frequency fluctuations) $\sigma_{ij}^2 = \sigma_i^2 + \sigma_j^2$. If we now let i = RMO-15 clock, and take j = Cs and Rb clocks in turn, then it is straightforward to obtain

$$\sigma_{RMO-15}^2 = \frac{1}{2}\left(\sigma_{\text{RMO-15,Cs}}^2 + \sigma_{RMO-15,Rb}^2 - \sigma_{Rb,Cs}^2\right). \quad (1)$$

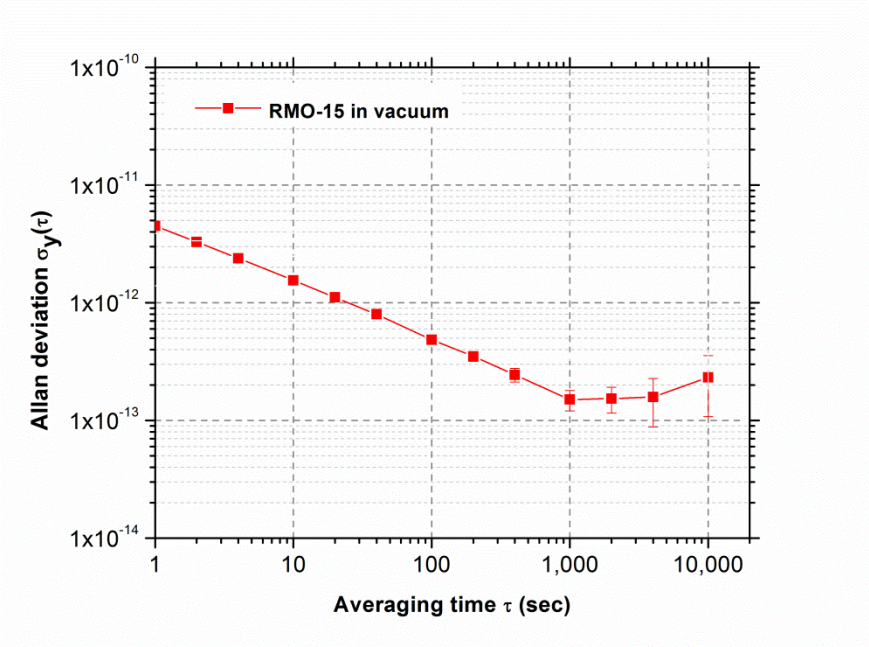

Figure 4. Measured Allan deviation of RMO-15 operating in vacuum.

In the following section, we will present two illustrative examples showing the general capabilities of our test station and the types of questions we can address. It is to be emphasized that none of the results we present below bears on the specific operational requirements or performance of the Milstar/AEHF system nor do the results bear on the specific capabilities of these devices as spacecraft atomic clocks. The results will simply demonstrate the type of information we can obtain with our simulation and test station, and the form of operational questions to address.

ILLUSTRATIVE RESULTS

ASSESSING OPERATIONAL ISSUES #1 – FREQUENCY RETRACE BETWEEN RMO MODE AND BACKUP MODE

A spacecraft RMO can be switched from its primary atomic-clock mode to a crystal-oscillator-backup mode and vice versa. In backup-mode the output frequency of the device derives from the quartz crystal oscillator in the RMO, but free-running (i.e., not tied to the atomic system). In atomic-clock mode, the quartz crystal is frequency-locked to the ground-state hyperfine splitting of ^{87}Rb as observed in an atomic

vapor. Following the switch, we monitored the clock frequency, the clock temperature, and all telemetry signals for approximately one-half hour, taking data every second. Figure 5 shows the frequency history of RMO-15 as it was commanded into RMO mode and backup mode ten times (where we have nominally set the RMO-mode frequency to zero). The shift in frequency between RMO mode and backup mode is due to the fact that the analog voltage (the "C-field" voltage), which was kept constant during the experiments, has different effects on the RMO frequency and the crystal oscillator frequency. Much more interesting are the spikes in frequency that appear when the clock was commanded to return to RMO mode. Note that these spikes are absent for the RMO-mode to backup-mode switch.

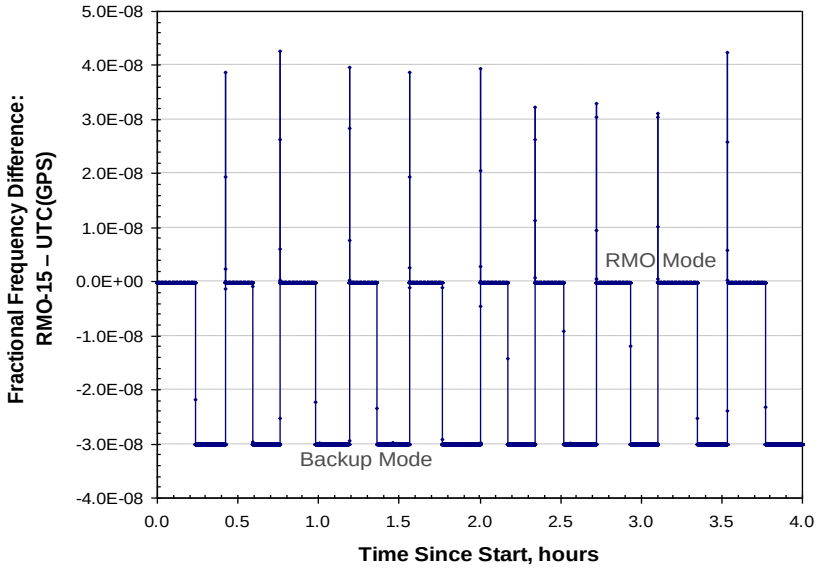

Figure 5. Frequency history of RMO-15 as it was sequentially commanded into RMO mode and backup mode ten times.

Figure 6 shows the data for all ten transitions overlapped in time. The data clearly show that the transient spikes are short-lived, and that the RMO frequency reaches equilibrium in roughly five seconds. Since the RMO-mode's frequency control loop has a finite time constant, the transient of Figure 6 is likely due to the temporal response of the control loop when the RMO is commanded back into RMO mode. The solid line corresponds to the response of a near-critically damped oscillator: $Ae^{-\gamma t}\cos(\omega t+\phi)$, with $A = 1.7\times10^{-7}$, $\gamma = 1$ sec^{-1}, $\omega = 0.8$ sec^{-1} and $\phi = 0.54\pi$, suggesting that the loop control time for RMO-15 is on the order of one second. Figure 7 displays the main results of this example, where we show the ability of the RMO to retrace its frequency when commanded into RMO mode (squares) and backup mode (circles). In the figure, zero corresponds to the mean value of all ten RMO-mode (or backup-mode) frequencies, and what is plotted is each measurement's deviation from that average. For each mode-switch, the last ten minutes of data prior to the next switch were used to compute an average clock frequency for that experimental trial; in that way, the clock always had about 20 minutes to equilibrate following a mode switch before we assessed its frequency. Error bars in the figure correspond to the standard deviation of the (roughly) 600 one-second frequency measurements that went into each trial's average. In the case of RMO mode, this standard deviation should, and does, correspond to the Allan deviation of the clock in RMO mode at one second. For backup mode, the standard deviation is larger than the clock's Allan deviation (in RMO mode) at one second. This is most likely due to the fact that deterministic variations (e.g., laboratory temperature, frequency drift) led to variations in crystal oscillator frequency over the measurement intervals.

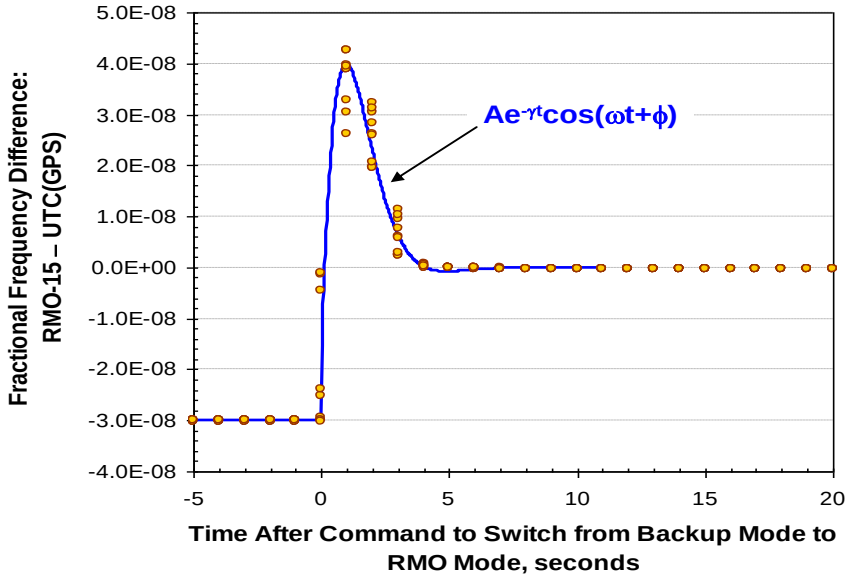

Figure 6. Transient frequency of RMO mode immediately after it is commanded to switch from backup mode to RMO mode.

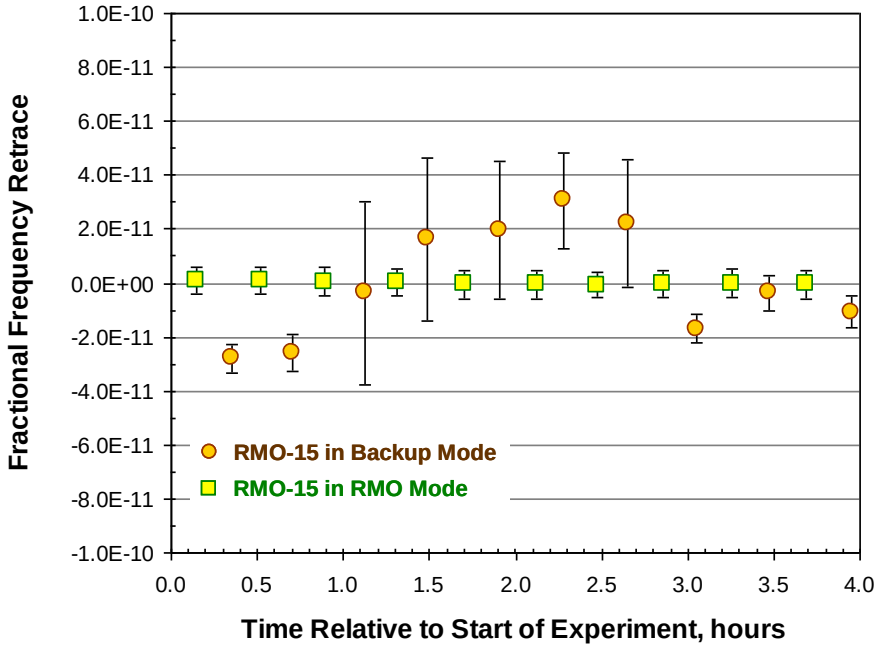

Figure 7. Frequency retrace for the clock operating in RMO mode (squares) and backup mode (circles).

Considering the deviations of the clock frequency from its average, the data of Figure 7 indicate that

- for RMO Mode: $\Delta f_{\text{retrace}} = \pm 6.4\times10^{-13}$;
- for Backup Mode: $\Delta f_{\text{retrace}} = \pm 2.1\times10^{-11}$.

Of these two, $\Delta f_{\text{retrace}}$ for RMO mode is likely the more important, since operators will typically be interested in knowing the nominal clock frequency on returning to RMO mode after some operational situation caused the operators to transition the RMO into backup mode.

ASSESSING OPERATIONAL ISSUES #2 – FREQUENCY EQUILIBRATION FOLLOWING A FREQUENCY UPDATE COMMAND

The RMO's frequency is tuned with a 16-bit frequency control word (FCW) ranging from 0000 to FFFF in hexadecimal numbers (0 to 65535 in decimal numbers). A built-in frequency update circuit converts the digital FCW to an analog voltage $V_{\text{C-field}}$ (called C-field voltage), acting on the clock's C-field solenoid coil. When the RMO is commanded from an initial frequency control word FCW_1 to a final word FCW_2, the C-field voltage, $V_{\text{C-field}}$, the current flowing through the C-field coil, $I_{\text{C-field}}$, and the power consumed by the coil, P_C (equivalent to the heating rate by the coil), change proportionally by:

$$\Delta V_{C-field} = k(FCW_2 - FCW_1) \tag{2}$$

$$\Delta I_{C-field} = \frac{k}{R_C}(FCW_2 - FCW_1) \tag{3}$$

$$\Delta P_C = \frac{k^2}{R_C}(FCW_2^2 - FCW_1^2) = \frac{k^2}{R_C}(FCW_1 + FCW_2)\Delta_{FCW} \tag{4}$$

Here, k is a proportionality constant, R_C is the resistance of the C-field coil, and $\Delta_{FCW} = (FCW_2 - FCW_1)$. Equation (4) suggests that the clock's internal thermal balance may be upset slightly by a change in the heating rate of the C-field coil, and as a consequence a new thermal equilibration will be established after the frequency update operation.

We first measured the output frequency of RMO-15 when it was tuned between FCW = 0000 and FFFF and found that the RMO's frequency undergoes a slow change before eventually stabilizing after the clock is tuned to FCW = FFFF. Alternatively, the clock's frequency seems to stabilize instantly when the clock is commanded back to FCW = 0000. Apparently, the slow change in the clock's frequency at FCW = FFFF results from an internal thermal equilibration process that takes place after a sudden increase in the RMO's C-field current. Figure 8 illustrates the measured fractional frequency of RMO-15 after it was tuned from FCW = 8000 (or 32768 in decimal) to FCW = FFFF (or 65535 in decimal), showing the slow frequency equilibration following the frequency-tuning command. We are able to fit the clock's fractional frequency y with an increasing exponential function of time t (in units of hour):

$$y(t) = 3.37\times10^{-8} - 1.9\times10^{-11}e^{-t/0.22} \tag{5}$$

The exponential fit gives an amplitude for the slow frequency change of $\Delta f / f_0 = 1.9 \times 10^{-11}$ and a 1/e (63%) time constant of $\tau = 0.22$ hours. After the RMO was fully stabilized at FCW = FFFF, we tuned the

clock back to FCW = 8000 and observed a reversed thermal equilibration as plotted in Figure 9. A decreasing exponential function fits the data as

$$y(t) = 6.68 \times 10^{-9} + 1.1 \times 10^{-11} e^{-t/0.17} \tag{6}$$

giving an amplitude for the frequency change of $\Delta f / f_0 = 1.1 \times 10^{-11}$ and a 1/e (63%) time constant of $\tau =$ 0.17 hours.

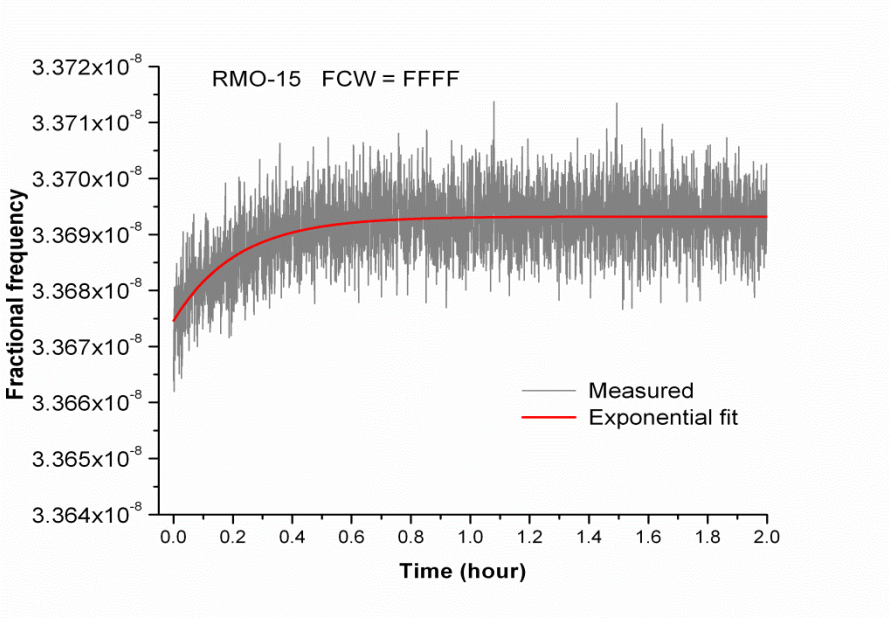

Figure 8. Measured frequency of RMO-15 when it is commanded from FCW = 8000 to FFFF.

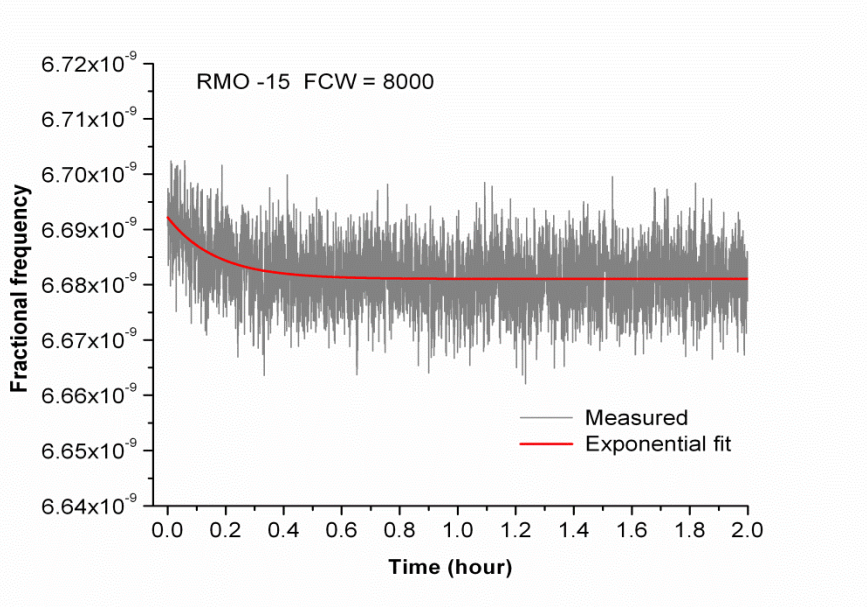

Figure 9. Measured frequency of RMO-15 when it is commanded back from FCW = FFFF to 8000.

From the above measurements we notice that the amplitude in Equation (6), $\Delta f / f_0 = 1.1\times10^{-11}$ for $FCW_{final} = 8000$, is approximately half the amplitude in Equation (5), $\Delta f / f_0 = 1.9\times10^{-11}$ for $FCW_{final} =$ FFFF. The 1/e time constants in both cases are almost the same (i.e., $\tau \cong 0.2$ hours). As depicted in Figure 8 and Figure 9, the complete equilibrium process lasts approximately one hour. After analyzing all the measured data, we obtained a first-order model suggesting that the amplitude of the fractional frequency change due to the post-tuning thermal equilibration is proportional to the *product* of the final frequency control word FCW_{final} and the FCW change Δ_{FCW} as described by Equation (7) and shown in Figure 10.

$$\frac{\Delta f}{f_0} = 9.8(5)\times10^{-21}\times FCW_{Final}\times\Delta_{FCW} \tag{7}$$

The linear dependence of $\Delta f/f_o$, on FCW_{final} in Equation (7) suggests that the frequency equilibration may be caused by a thermally-induced slow change in the clock's effective C-field strength. This mechanism suggests itself because the clock's magnetic field sensitivity is a linear function of the C-field strength, $\partial f/\partial B \propto B$ **[10]**, explaining why a frequency change could hardly be observed when the RMO was commanded to FCW = 0000. However, we are at present unable to explain how the thermal equilibration process affects the clock circuitry and the effective C-field strength. We note, however, that the process is not as simple as a temperature-induced change in the C-field coil resistance. Based on the measurements, we expect the C-field coil's impedance to increase with temperature, which in turn would imply that Figure 8 should show a decreasing exponential and Figure 9 an increasing exponential. Nonetheless, our study provides a first-order model that can be employed to estimate the thermal equilibration changes in clock frequency following a frequency tuning command.

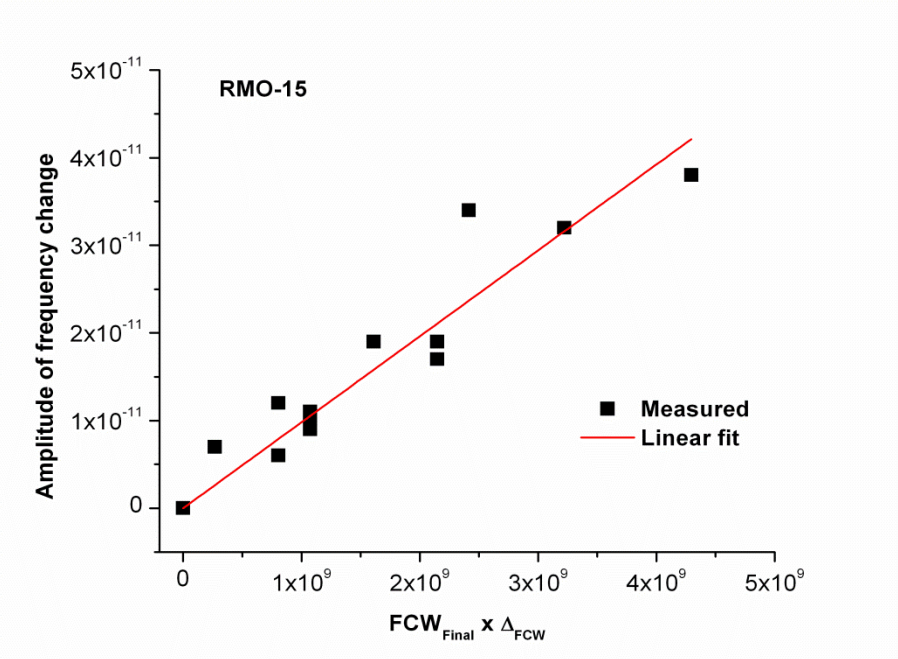

Figure 10. Measured amplitudes (black squares) of the thermal equilibration induced frequency change as a function of the product of FCW_{final} and Δ_{FCW} (in decimal numbers). The red line is a linear fit.

To further examine the impact of this post-tuning thermal equilibration on the RMO's frequency stability, we measured the clock's Allan variance when RMO-15 was commanded to various frequency control words. Our results show that the RMO can always re-stabilize and re-gain the expected frequency stability after a one hour thermal equilibration period. As demonstrated in Figure 11, the blue-squares correspond to the Allan deviation of RMO-15 calculated using the full data set of 91 hours right after the RMO was tuned to FCW = FFFF. Due to the thermal equilibration, the clock's Allan deviation behaves abnormally for averaging times $\tau > 400$ s. To compare, the red-dots give the Allan deviation calculated using data that excludes the thermal equilibration (i.e., we only include frequency data points for $t > 1$ hour). The Allan variance now behaves normally. Furthermore, if we wait for 24 hours (i.e., we only include data for $t > 24$ hours in the analysis), the black-squares indicates that the RMO appears completely unaffected by the thermal equilibration.

It is important to note that the situation discussed here (i.e., changing the RMO's control word by nearly half its full tuning range), is extremely non-operational, and what the RMO was never intended for. In addition, under normal situations, our data demonstrate that any frequency equilibration following a frequency control-word change will be insignificant and ignorable. This is especially true when the RMO operates at low FCW settings, and the frequency update operation only involves a normal (i.e., small) changes in clock frequency. Nevertheless, it is just this type of information that operational personnel find useful as they attempt to understand the spacecraft timekeeping.

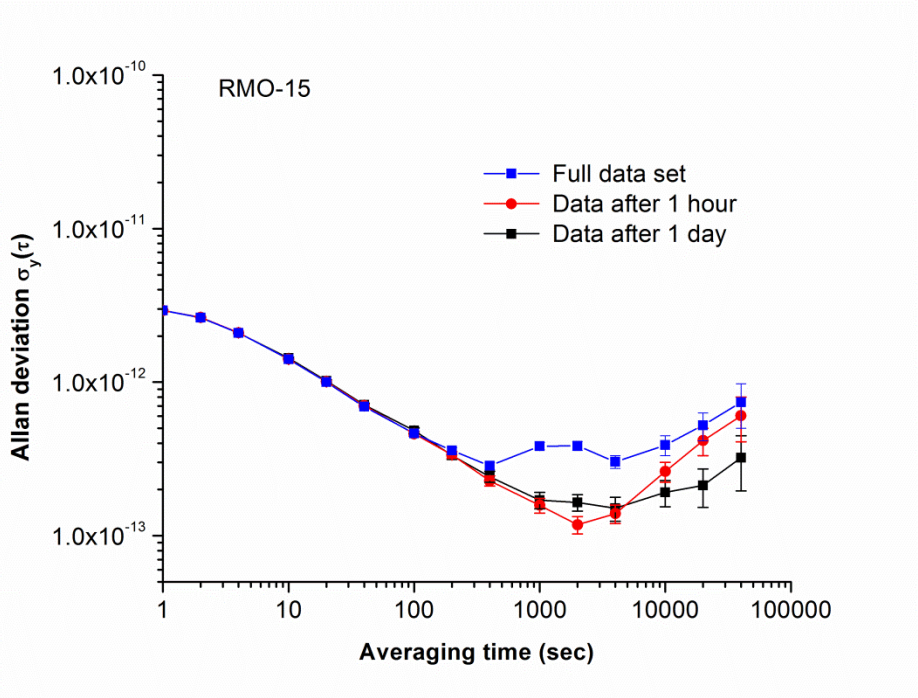

Figure 11. Allan deviations of RMO-15 operating at FCW = FFFF. The frequency measurement starts right after the RMO is commanded from FCW = 8000 to FFFF.

SUMMARY

In order to help satellite operators understand and resolve flight atomic clock issues, we have constructed an atomic clock flight simulation and test station, and have assessed and investigated the behavior of two Milstar rubidium master oscillators in a simulated space environment. To illustrate the capability of the

test facility, we have presented two examples: 1) measurements of frequency retrace uncertainty between RMO mode and backup mode and 2) observations of the frequency equilibration process following a frequency update command. These examples have demonstrated that our simulation and test station is able to address operation-related questions, whose answers may not exist in pre-flight test data archives. In addition, systems engineers will find our results useful, since we can provide realistic parameters for their numerical simulation of system performance **[5, 11]**.

REFERENCES

[1] L. L. Lewis, 1991, *"An introduction to frequency standard,"* **Proc. IEEE 79**(7), pp. 927-935.

[2] J. Camparo, 2007, "The *rubidium atomic clock and basic research,"* **Physics Today, 60**(11), 33-39.

[3] M. Weiss, P. Shome and R. Beard, 2006, *"GPS signal integrity dependences on atomic clocks,"* in Proc. 38th Annual Precice Time and Time Interval (PTTI) Systems and Applications Meeting (US Naval observatory, Washington, DC), pp. 439-448.

[4] R. T. Dupuis, T. J. Lynch and J. R. Vaccaro, 2008, *"Rubidium frequency standard for the GPS IIF program and modifications for the RAFSMOD program,"* in Proc. of 2008 IEEE International Frequency Control Symposium (IEEE Press, Piscataway, NJ), pp. 655-660.

[5] J. C. Camparo, Y. Chan and R. P. Frueholz, 2000, *"Space-segment timekeeping for next generation Milsatcom,"* in Proc. 31st Annual Precice Time and Time Interval (PTTI) Systems and Applications Meeting (US Naval Observatory, Washington, DC), pp. 121-132.

[6] J. C. Camparo, R. P. Frueholz and A. P. Dubin, 1997, *"Precise time synchronization of two Milstar communication satellites without ground intervention,"* **International Journal of Satellite Communication, 15**, 135-139.

[7] S. D. Lalumondiere, S. C. Moss and J. C. Camparo, 2003, *"A 'space experiment' examining the response of a geosynchronuous quartz crystal oscillator to various levels of solar activities,"* **IEEE Trans. Ultrasonic, Ferroelectric, Frequency Control, 50**(3), 210-213.

[8] J. E. Gray and D. W. Allan, 1974, *"A method for estimating the frequency stability of an individual oscillator,"* in Proc. 28th Annual Frequency Control Symposium (IEEE Press, Piscataway, NJ), pp. 243-246.

[9] C. Audoin and B. Guinot, 2001, **The measurement of time: time, frequency and atomic clock** (Cambridge University Press, New York, NY).

[10] F. G. Major, 1998, **The quantum beat: the physical principles of atomic clocks** (Springer-Verlag, New York, NY).

[11] Y. Chan, J. C. Camparo, and R. Frueholz, *"The autonomous detection of clock problems in satellite timekeeping systems,"* in Proc. 31st Annual Precise Time and Time Interval (PTTI) Systems and Applications Meeting, Dana Point, CA, 1999, (United States Naval Observatory, Washington, DC, 2000), pp. 111-120.